Optik - International Journal for Light and Electron Optics 252 (2022) 168531

Contents lists available at ScienceDirect

Optik

journal homepage: www.elsevier.com/locate/ijleo

Design and implementation of passive speckle reduction in laser projector with refractive optical element and lenslet integrator

Zhaomin Tong [a,b,*], Changyuan Sun [a,b], Yifei Ma [a,b], Mei Wang [a,b], Suotang Jia [a,b], Xuyuan Chen [a,b,c]

[a] State Key Laboratory of Quantum Optics and Quantum Optics Devices, Institute of Laser Spectroscopy, Shanxi University, Taiyuan, Shanxi 030006, China
[b] Collaborative Innovation Center of Extreme Optics, Shanxi University, Taiyuan, Shanxi 030006, China
[c] Department of Microsystems, University of South-Eastern Norway, Borre N-3184, Norway

ARTICLE INFO

Keywords:
Refractive optical element
Lenslet integrator
Passive speckle reduction
Laser projection displays

ABSTRACT

A refractive optical element (ROE), together with a lenslet integrator (LI), is designed for passive speckle reduction in laser projection displays. ROE cells create optical path differences among laser sub-beams, and consequently destroy laser temporal and spatial coherences when the partially correlated laser sub-beams are superposed by the LI. By using the ROE and the LI, objective and subjective speckle contrasts are reduced to 0.18 and 0.2, respectively. The demonstrated passive speckle reduction technique does not require the use of motors, which shows superiorities over other speckle reduction methods by changing diffuser etc.

1. Introduction

After the invention of lasers in 1960s, the work of developing more vivid and brighter mercury-free displays by red, green and blue lasers is continuously in progress [1]. It is in recent years that the commercialization of laser displays is boosted mainly attributing to the success of the development of high-power and low-cost laser diodes, especially for the green and red colors [2,3]. Speckle, which results in poor image quality in laser displays, on the other hand, though has been claimed by many laser projector manufactures being solved, problems exist for the adopted speckle reduction methods.

Changing diffuser is a typical speckle reduction technique [4–6]. Different speckles form when a diffuser is vibrating or rotating, and thus reduces speckle by the summation of different speckle patterns. Speckle contrast can be reduced from one to $1/(2\ T)^{1/2} = (\lambda Z/2Dvt)^{1/2}$ by the changing diffuser, where T represents the temporal degree of speckle reduction freedom, v is traveling velocity and t is camera exposure period, λ, Z and D are laser wavelength, image distance and diameter of the imaging lens, respectively, and the factor of two is attributed to the depolarization by the screen [7]. According to the aforementioned relationship, changing diffuser can easily reduce speckle down to contrasts lower than 0.05, which are the values that speckle cannot be recognized by human eyes [8]. However, due to the finite temporal integration time of human eyes (50 ms), high-speed motors are required to actuate the diffuser, which are bulky and noisy and cause extra electric energy consumption. In one speckle-reduced laser projection system by changing diffuser, a micro-vibrated diffuser is used as the paper screen [9]. It is unpractical in consideration of cinema screens etc., where

* Corresponding author at: State Key Laboratory of Quantum Optics and Quantum Optics Devices, Institute of Laser Spectroscopy, Shanxi University, Taiyuan, Shanxi 030006, China.
E-mail address: zhaomin.tong@sxu.edu.cn (Z. Tong).

https://doi.org/10.1016/j.ijleo.2021.168531
Received 23 September 2021; Received in revised form 3 December 2021; Accepted 22 December 2021
Available online 27 December 2021

high-power actuators are demanded to vibrate the large-sized screen. A coexisting consequence for changing diffuser is light scattering when a moving diffuser is placed within the projection system. Etendue is increased by the scattered lights, which may cause extra optical power loss. The application of the moving diffuser within the projection system also induces the formation of compound speckles on the screen [7]. The compound speckles have a higher contrast because the contrast of the reduced compound speckles is determined both by the temporal and spatial degrees of speckle reduction freedom [7]. Normally, the value of the spatial degree of speckle reduction freedom is low (lower than one hundred), which makes the compound speckles on the screen have a higher contrast [10].

Laser linewidth broadening and wavelength diversity are another two commonly used speckle reduction methods, which are based on the suppression of laser temporal coherence [11–15]. Laser diodes have a typical full-width-half-maximum linewidth of several nanometers, which constrains the speckle reduction efficiency achieved by laser linewidth broadening. Wavelength diversity can be realized by employing laser diodes with different primary wavelengths. For a single laser diode, one can also achieve wavelength diversity by modulating its drive current, i.e., by obtain independent longitudinal modes (multimode) that arise from mode hopping [16]; the modulation period of the laser diode drive current shall be short, specifically, within the temporal integration time of human eyes, which in turn requires the design of high-speed electronic driver circuit. Another issue for wavelength diversity is that speckle cannot be reduced effectively. Assuming that M laser diodes with fully uncorrelated primary wavelengths or a laser diode with M fully uncorrelated modes are introduced, speckle can be reduced by $1/M^{1/2}$ [7]. Currently Nichia and OSRAM etc. laser diode manufactures only supply few types of RGB laser diodes emitting different primary wavelengths, and the obtainable number of independent longitudinal modes by modulating the drive current of the laser diode is low. Therefore, the achievable maximum value of N is restricted.

In this paper, we use a refractive optical element (ROE) and a lenslet integrator (LI) to suppress laser temporal and spatial coherences and to reduce speckle passively. The ROE has a staircase-like structure, which introduces different optical path lengths when laser sub-beams transmit through. The optical path differences among the laser sub-beams destroy the temporal coherence of a laser diode, and with the help of the LI to convert a Gaussian beam profile into a uniform flat-top light distribution, the spatial coherence of the laser diode is destroyed. This mechanism is simulated in Zemax and verified by experimental results.

2. Design and simulation

In projection displays, a uniform rectangular illumination light field is needed. This requirement can be accomplished by using an optical homogenizer such as a light pipe based on multiple total internal reflections or a LI based on the principle of Köhler illumination [17]. When the sizes of microdisplay panels are large, cross-sections of light pipes are approximately the same as the sizes of the microdisplay panels, which consequently demand light pipes having very long lengths to obtain good light field homogenization. Under such a circumstance, homogenizers using LIs are preferred because they are more compact.

Fig. 1 shows simulation model in Zemax, which is also consistent with experimental setup for objective speckle measurement. A 50 mW multimode laser diode with thermal-controlled mount is used as illumination light source. The driving current and working temperature of the laser diode are constant values of 150 mA and 20 °C, respectively. The central wavelength of the laser diode is $\lambda =$ 520 nm. The laser beam is collimated by a freeform lens embedded inside the thermal-controlled mount. The collimated circular laser beam is expanded by a beam expander to 40 mm in diameter. An adjustable iris is employed to change the effective laser beam diameter ranging from 5 mm to 35 mm, where the largest laser beam diameter is determined by the working area of the lenslet arrays. A ROE is placed closely after the iris. We have used a LI composed of a pair of lenslet arrays and an auxiliary lens for light field homogenization purpose. There are 10 × 13 lenslets for the lenslet array, where each lenslet has a focal length of $f_{LA} = 38.1$ mm, a width of $W_{LA} = 4$ mm, and a height of $H_{LA} = 3$ mm. The lenslet arrays and the auxiliary lens are arranged in a standard style to obtain a uniform flat-top light distribution by the superposition of laser sub-beams determined by the lenslets [17]. A sandblasted glass diffuser is placed at the focal plane of the auxiliary lens, where the focal length of the auxiliary lens is $f_{AL} = 100$ mm. Therefore, the width and height of the homogenized flat-top beam profile are $W_{FT} = f_{AL} \times W_{LA}/f_{LA} = 10.5$ mm and $L_{FT} = f_{AL} \times H_{LA}/f_{LA} = 7.9$ mm, respectively [17]. A charge-coupled device camera is used to capture objective speckles, where the exposure time of the camera is changed accordingly to make sure that the image sensors work in their linear region when the diameter of the iris is adjusted. In order to make the size of objective speckles significantly larger than camera pixel size, the distance from the diffuser to the camera is set as 1000 mm.

ROE fabrication has been reported elsewhere [18,19]. In brief, two groups of glasses are assembled along orthogonal directions onto a transparent glass substrate by ultraviolent glue. The lengths of the glasses are the same, which are 80 mm. In order to match with the 4 mm × 3 mm lenslet planar dimensions, widths of the horizontally and vertically posited glasses are designed as 4 mm and 3 mm, respectively. The heights of the two groups of glasses are different, varying from 0.5 mm to 6 mm with an even increment of

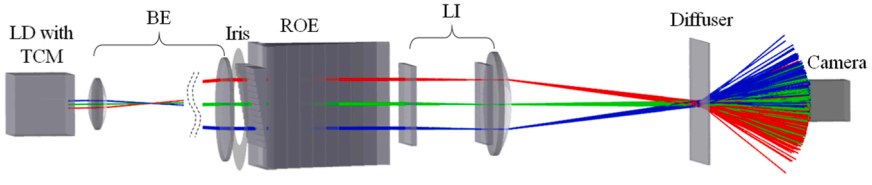

Fig. 1. Simulation model and experimental setup for objective speckle measurement, where the colored lines shown in the figure represent different parts of the laser beam. LD: laser diode, TCM: thermal-controlled mount, BE: beam expander, ROE: refractive optical element, LI: lenslet integrator.

0.5 mm for the vertically aligned group and from 6.5 mm to 58.5 mm with an even increment of 6.5 mm for the horizontally aligned group. Therefore, we obtain staircase-like structures with heights ranging from 0 mm to 64.5 mm, where the heights between two adjacent ROE cells have an even increment of 0.5 mm. Here, it should be known that the optical axis in Fig. 1 passes through both the centers of the sixth row and sixth column ROE cell and the sixth row and sixth column lenslets.

We have used sequential mode in Zemax to calculate the optical path differences produced on the diffuser among the laser sub-beams, where the refractive index of the glasses is defined as 1.46. Fig. 2 presents simulation results before and after introducing the ROE, where the effective laser beam diameter is set as 35 mm. Here, the reference laser sub-beam is the one passing through the optical axis.

As shown in Fig. 2, the mean optical path differences between two adjacent laser sub-beams are 10 μm and 228 μm before and after introducing the ROE, respectively. Thus, we can conclude that the optical path differences among the laser sub-beams are improved after introducing the ROE.

3. Experimental results and discussions

3.1. Objective speckle

We have used experimental setup shown in Fig. 1 to measure objective speckles. Fig. 3 shows experimental results about the relationships between objective speckle contrast C and the equivalent number of independent speckle patterns N_e and the diameter of the iris before and after introducing the ROE. Objective speckle contrast C and the equivalent number of independent speckle patterns N_e are calculated by using [7].

$$C = \frac{\langle I \rangle}{\sigma}, \tag{1}$$

$$N_e = \left(\frac{C_b}{C_a}\right)^2, \tag{2}$$

where $<I>$ and σ represent the mean value and standard deviation of speckle intensity, respectively, and C_b and C_a are objective speckle contrasts before and after speckle reduction, respectively.

As shown in Fig. 3, the initial objective speckle contrast is 0.77 for the iris diameter of 3 mm. The planar dimensions of the lenslets are 4 mm × 3 mm, and the widths of the horizontally and vertically posited glasses to compose ROE are 4 mm and 3 mm, respectively, thus there is no spatial integration when the diameter of the iris is 3 mm because the effective laser beam only transmits through a single lenslet and a single ROE cell. In this situation, no speckle reduction mechanisms are introduced except the depolarization caused by the diffuser. In theory, if the diffuser can fully depolarize scattered lights, the initial speckle contrast shall be $1/2^{1/2} = 0.71$ because of the two degrees of speckle reduction freedom provided by the diffuser depolarization [7]. The obtained initial speckle contrast of 0.77 can be attributed to partial depolarization of the diffuser. When the diameter of the iris is increased, objective speckle contrast starts to decrease, where objective speckle contrast is reduced more rapidly with the ROE and the LI than only with the LI. For the largest iris diameter of 35 mm, the minimum objective speckle contrasts are 0.32 and 0.18 before and after using the ROE, respectively. This is in agreement with the simulated optical path differences presented in Fig. 2, where optical path differences are greatly improved by introducing the ROE.

In Fig. 3, it can also be found that the equivalent numbers of independent speckle patterns N_e are improved by using the combination of the ROE and the LI, where the maximum values are 5.6 by using the LI and 17.7 by using the ROE and the LI in Fig. 3. The superposition of N speckle patterns results in a speckle contrast C_a equaling to

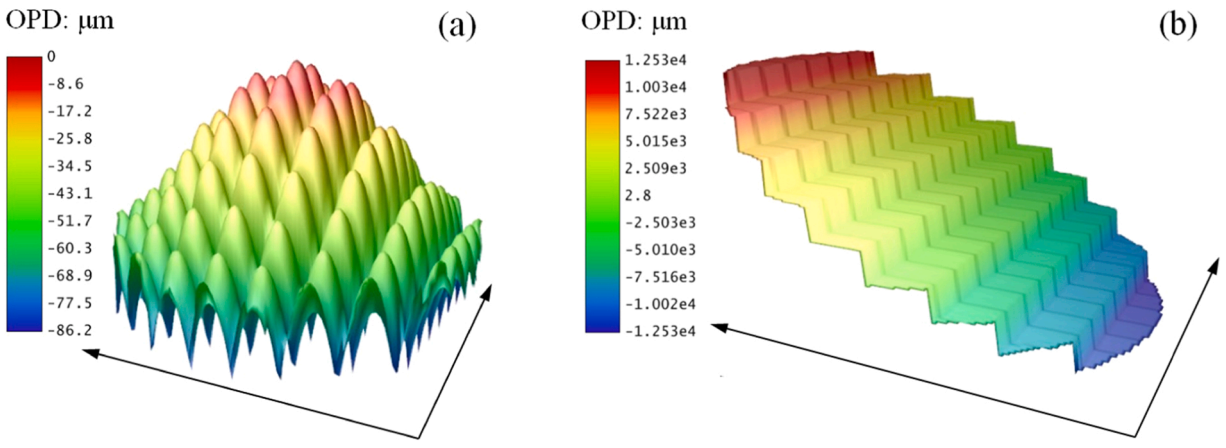

Fig. 2. Simulated optical path differences produced on the diffuser among the laser sub-beams (a) before and (b) after introducing the ROE.

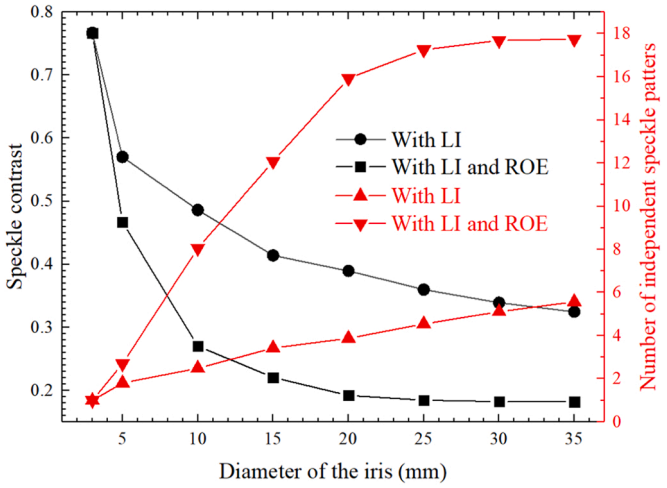

Fig. 3. Relationship between objective speckle contrast and the equivalent number of independent speckle patterns and the diameter of the iris before and after introducing the ROE.

$$C_a = \frac{\sqrt{\sum_{i=1}^{N}\sum_{j=1}^{N}\left[\overline{I_i I_j} + \rho_{i,j}\sqrt{\overline{(I_i - \overline{I_i})^2}\,\overline{(I_j - \overline{I_j})^2}}\right] - \left(\sum_{j=1}^{N}\overline{I_j}\right)^2}}{\sum_{j=1}^{N}\overline{I_j}}, \tag{3}$$

where $\rho_{i,j}$ is the correlation coefficient of the ith and jth speckle patterns, and I_i and I_j are the light intensities of the ith and jth speckle patterns, respectively [20]. When larger optical path differences are introduced by the laser sub-beams, the correlation coefficients of the speckle patterns produced by these laser sub-beams decrease, and the speckle contrast of the superposed speckle image becomes lower. In principle, if all the laser sub-beams transmits through the ROE and the lenslets are uncorrelated, the equivalent number of independent speckle patterns N_t shall be [18].

$$N_t = \frac{\left(\sum_{n=1}^{N} I_n\right)^2}{\sum_{n=1}^{N} I_n^2}, \tag{4}$$

where I_n is the light intensity of the nth speckle pattern, and N is the number of uncorrelated laser sub-beams. When the iris diameter is 35 mm, the effective laser beam illuminates sixty-one ROE cells and the corresponding lenslets entirely, and thus the value of N_t shall be larger than sixty-one. There are mainly two aspects making the equivalent numbers of independent speckle patterns obtained from experiment being lower than expectations, i.e., $N_e < N_t$. Firstly, the minimum optical path differences among adjacent laser sub-beams are shorter than the coherence length of the laser diode, where the laser diode has a coherence length of about 350 μm [18]. The spectrum of the multimode laser diode has a number of longitudinal modes with narrow bandwidth, which makes the formation of a number of peaks within the envelope of the absolute value of the complex degree of temporal coherence [21]. As shown in Fig. 2(b),

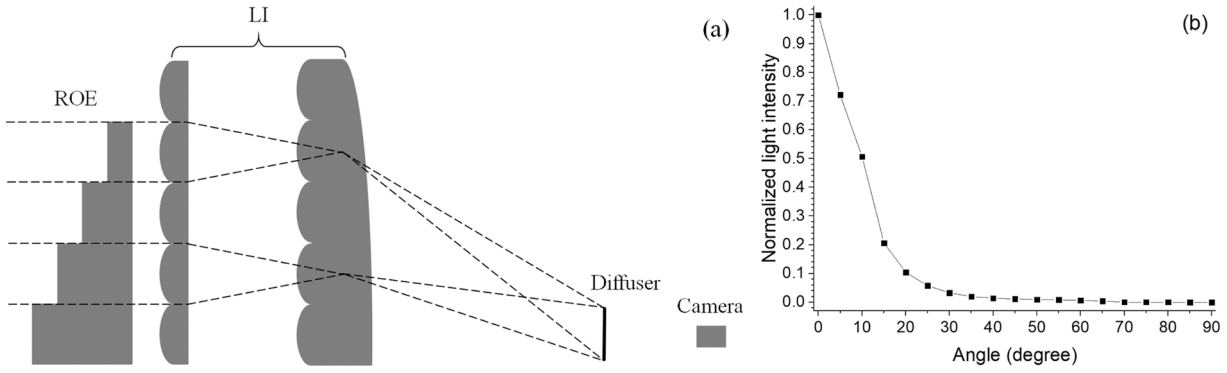

Fig. 4. An example to explain the superposition of laser sub-beams transmitting through the ROE and the LI (a), and the scattering property of the diffuser. ROE: refractive optical element, LI: lenslet integrator.

the mean optical path difference between two adjacent laser sub-beams is 228 μm after introducing the ROE. The mean optical path difference between two adjacent laser sub-beams is comparable to the coherence length of the laser diode, and the absolute value of the complex degree of temporal coherence is low when the ROE is used. Therefore, the temporal and spatial coherences of the laser diode are partially destroyed by the optical path differences brought by the laser sub-beams. Secondly, the laser sub-beams illuminates the diffuser along different directions, and the scattering angle of the diffuser is very small, which together make laser sub-beams have unequal contributions to speckle reduction. Fig. 4(a) schematically shows an example when two laser sub-beams transmit through the ROE cells and the LI, and Fig. 4(b) shows the scattering angle measurement result of the diffuser.

As shown in Fig. 4(a), the angle of incidence of the mth laser sub-beam can be calculated approximately by $\theta_m = \tan^{-1}(mH_{LA}/f_{AL})$, where m are integers ranging from -6 to 6. Therefore, the angles of incidence of the laser sub-beams are varying from -10.2° to 10.2°, respectively, and the angles of incidence between the mth and $(m+1)$th laser sub-beams have an interval of about $\Delta\theta = 1.7^\circ$. According to Eq. (4), when uncorrelated speckle patterns are summed, the equivalent number of independent speckle patterns is influenced by the intensities of individual speckle patterns. If the intensities of the superposed uncorrelated speckle patterns are not equal, speckle reduction becomes less efficient, and the equivalent number of independent speckle patterns is lower than the number of the superposed uncorrelated speckle patterns. In Fig. 4(b), we can find that the diffuser has a full-width-half-maximum scattering angle at about 10°. Therefore, when the laser sub-beams illuminate the diffuser along different directions with the angles of incidence ranging from -10.2 to 10.2°, the contribution of each laser sub-beam on the superposed speckles that are perceived by the 4.76 mm × 3.57 mm sensing area of the camera are unequal. Because of the aforementioned two aspects, the equivalent numbers of independent speckle patterns obtained from experiment are lower than expected values.

Another observation from Fig. 3 is the saturations of objective speckle contrasts and the equivalent number of independent speckle patterns when the diameter of the iris is very large. This result can also be explained by the scattering angle measurement presented in Fig. 4(b). When the diameter of the iris becomes larger, the contributions of the light intensities from the newly introduced laser sub-beams on the camera become weaker because these laser sub-beams have larger absolute values of angles of incidence on the diffuser. The camera perceives less light intensities from the outer laser sub-beams, and thus the decreasing rate of objective speckle contrasts and the increasing rate of the equivalent number of independent speckle patterns become saturated.

3.2. Subjective speckle

A laser projection system using an ultra-short throw lens is designed to demonstrate speckle reduction realized by the ROE and the LI. Fig. 5(a) shows the laser projection system, and Fig. 5(b) and 5 (c) present subjective speckle images before and after introducing the ROE, where the iris diameter is 35 mm.

In Fig. 5, similar optical setup as Fig. 1 is adopted before a transparent plastic. The transparent plastic is placed in the plane where homogenized optical field is generated by the LI. A letter "S" is painted on the transparent plastic, which is projected by the ultra-short throw lens to a screen. The charged-coupled device camera is mounted with an imaging lens to capture subjective speckles, where the imaging lens has a focal length of 75 mm, and the distance from the imaging lens to the screen is 100 mm to record subjective speckles properly.

Subjective speckle contrasts are calculated by using Eq. (1), where these values are 0.33 for Fig. 5(b) and 0.2 for Fig. 5(c). Comparing with the corresponding objective speckle contrasts, these values are higher. The differences between objective speckle contrasts and subjective speckle contrasts can be explained by compound speckle theory [7,22]. Besides the speckles formed on the screen, there are other existing interferences and speckles in the laser projection system shown in Fig. 5(a) because of the imperfect

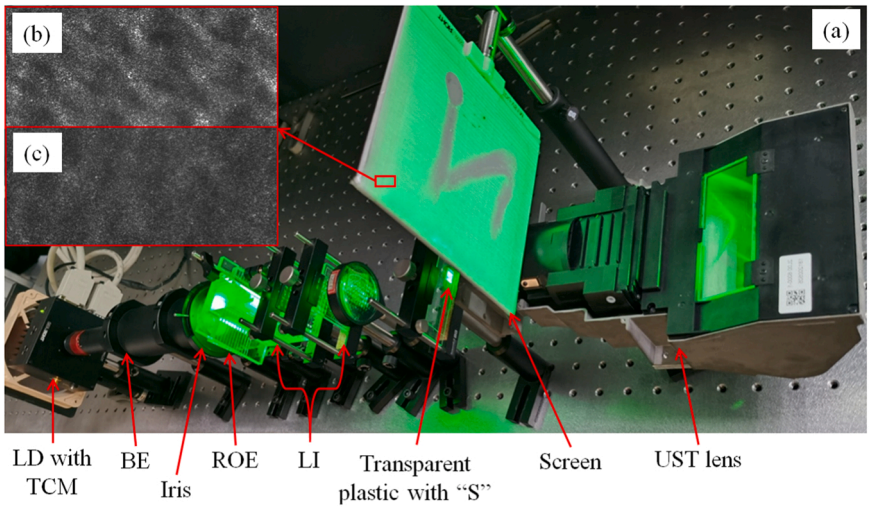

Fig. 5. Speckle reduced laser projection system (a), and subjective speckle images before (b) and after introducing the ROE. LD: laser diode, TCM: temperature-controlled mount, BE: beam expander, ROE: refractive optical element, LI: lenslet integrator, UST: ultra-short throw.

smooth surface of the transparent plastic. The speckles formed on the transparent plastic are enlarged by the ultra-short throw lens onto the screen, and thus we can observe small-sized speckles lying inside large-sized speckles in Fig. 5(b) and 5 (c), i.e., compound speckles. Because $[(S+T\pm1)/2ST]^{1/2}$ is always larger than $T^{1/2}$, the speckle contrast of a compound speckle pattern is always higher than that of the speckle pattern where first speckles form [7,22].

One should know that in a real laser projector, the transparent plastic in Fig. 5(a) can be replaced by display chips such as a digital micromirror device or a liquid crystal on silicon. In this situation, the subjective speckle contrast in Fig. 5(b) and 5 (c) shall be more close to objective speckle contrasts obtained in Fig. 3 under the same iris diameter.

4. Conclusions

In conclusion, we have demonstrated a passive speckle reduction method for laser projection application using a ROE together with a LI. Both objective speckle and subjective speckle are investigated before and after using the ROE. Experimental results show the combination of the ROE and the LI can effectively reduce speckle, and speckle reduction efficiency can be improved by introducing more partially correlated laser sub-beams with the ROE and LI cells. In comparison with other speckle reduction techniques such as a changing diffuser, the proposed passive speckle reduction method does not require motors to drive the diffuser, thus, it has zero electric energy consumption. In order to reduce speckle more effectively, the ROE and the LI can work together with other independent speckle reduction mechanisms, e.g., wavelength diversity, to obtain lower speckle contrasts.

Declaration of Competing Interest

The authors declare that they have no known competing financial interests or personal relationships that could have appeared to influence the work reported in this paper.

Acknowledgments

National Key Research and Development Program of China (2016YFB0401903); Natural Science Foundation of Shanxi Province (201901D111024); Changjiang Scholars and Innovative Research Team in University of Ministry of Education of China (IRT_17R70); State Key Program of National Natural Science Foundation of China (11434007); 111 Project (D18001); Fund for Shanxi "1331 Project" Key Subjects Construction.

References

[1] K. Chellappan, E. Erden, H. Urey, Laser-based displays: a review, Appl. Opt. 49 (25) (2010) F79–F98.
[2] M. Murayama, Y. Nakayama, K. Yamazaki, Y. Hoshina, H. Watanabe, N. Fuutagawa, H. Kawanishi, T. Uemura, H. Narui, Watt-class green (530 nm) and blue (465 nm) laser diodes, Phys. Status Solidi A 215 (2018), 1700513.
[3] T. Nishida, K. Kuramoto, Y. Iwai, T. Fujita, T. Yagi, Multi-emitter 638-nm high-power broad area laser diodes for display application, Proc. SPIE 10939 (2019), 109391H.
[4] G. Li, Y. Qiu, H. Li, Coherence theory of a laser beam passing through a moving diffuser, Opt. Express 21 (11) (2013) 13032–13039.
[5] J. Pan, C. Shih, Speckle noise reduction in the laser mini-projector by vibrating diffuser, J. Opt. 19 (2017), 045606.
[6] T. Stangner, H. Zhang, T. Dahlberg, K. Wiklund, M. Andersson, Step-by-step guide to reduce spatial coherence of laser light using a rotating ground glass diffuser, Appl. Opt. 56 (19) (2017) 5427–5435.
[7] J. Goodman, Speckle Phenomena in Optics: Theory and Applications, Englewood, Colorado, 2006.
[8] S. Roelandt, Y. Meuret, G. Craggs, G. Verschaffelt, P. Janssens, H. Thienpont, Standardized speckle measurement method matched to human speckle perception in laser projection systems, Opt. Express 20 (8) (2012) 8770–8783.
[9] S. Tu, H. Lin, M. Lin, Efficient speckle reduction for a laser illuminating on a micro-vibrated paper screen, Appl. Opt. 53 (22) (2014) E38–E46.
[10] M. Brennesholtz, E. Stupp, Projection Displays, second ed., 2008.
[11] N. Yu, J. Choi, H. Kang, D. Ko, S. Fu, J. Liou, A. Kung, H. Choi, B. Kim, M. Cha, L. Peng, Speckle noise reduction on a laser projection display via a broadband green light source, Opt. Express 22 (3) (2014) 3547–3556.
[12] Q. Ma, C. Xu, Wavelength blending with reduced speckle and improved color for laser projection, Opt. Lasers Eng. 97 (2017) 27–33.
[13] H. Yamada, K. Moriyasu, H. Sato, H. Hatanaka, Effect of incidence/observation angles and angular diversity on speckle reduction by wavelength diversity in laser projection systems, Opt. Express 25 (25) (2017) 32132–32141.
[14] H. Yamada, K. Moriyasu, H. Sato, H. Hatanaka, K. Yamamoto, Theoretical calculation and experimental investigation of speckle reduction by multiple wavelength lasers in laser projector with different angular diversities, J. Opt. 21 (2019), 045602.
[15] S. Lee, D. Kim, S. Nam, B. Lee, J. Cho, B. Lee, Light source optimization for partially coherent holographic displays with consideration of speckle contrast, resolution, and depth of field, Sci. Rep. 10 (2020) 18832.
[16] I. Yılmazlar, M. Sabuncu, Speckle noise reduction based on induced mode hopping in a semiconductor laser diode by drive current modulation, Opt. Laser Technol. 73 (2015) 19–22.
[17] R. Voelkel, K. Weible, Laser beam homogenizing: limitations and constraints, Proc. SPIE 7102 (2008) 71020J.
[18] Z. Tong, C. Sun, Y. Ma, M. Wang, S. Jia, X. Chen, Laser spatial coherence suppression with refractive optical elements toward the improvement of speckle reduction by light pipes, IEEE Access 7 (2019) 172190–172198.
[19] Z. Tong, F. Niu, Z. Jian, C. Sun, Y. Ma, M. Wang, S. Jia, X. Chen, Microrefractive optical elements fabricated by multi-exposure lithography for laser speckle reduction, Opt. Express 28 (23) (2020) 34597–34605.
[20] Z. Tong, S. Song, S. Jia, X. Chen, Nonsequential speckle reduction method by generating uncorrelated laser subbeams with equivalent intensity using a reflective spatial light modulator, IEEE Photonics J. 9 (2017), 7000508.
[21] D. Lee, C. Jang, K. Bang, S. Moon, G. Li, B. Lee, Speckle reduction for holographic display using optical path difference and random phase generator, IEEE T. Ind. Inform. 15 (2019) 6170–6178.
[22] Z. Tong, X. Chen, M. Akram, A. Aksnes, Compound speckle characterization method and reduction by optical design, J. Disp. Technol. 8 (3) (2012) 132–137.